Japanese Journal of Ophthalmology (2019) 63:234–242
https://doi.org/10.1007/s10384-019-00657-8

THE OFFICIAL INTERNATIONAL JOURNAL OF THE JAPANESE OPHTHALMOLOGICAL SOCIETY

CLINICAL INVESTIGATION

Three-dimensional analysis of morphologic changes and visual outcomes in diabetic macular edema

Hyungwoo Lee[1] · Kyung Eun Kang[1] · Hyewon Chung[1] · Hyung Chan Kim[1]

Received: 31 May 2018 / Accepted: 21 December 2018 / Published online: 19 February 2019

Abstract

Purpose To investigate the association of retinal fluid volume with the visual and anatomic outcomes of patients with diabetic macular edema (DME) after treatment with bevacizumab.

Study design Retrospective observational study.

Methods We retrospectively analyzed 65 eyes of 58 DME patients treated with bevacizumab. The volumes of the inner intraretinal fluid (IRF) in the inner nuclear layer (INL), outer IRF in the outer plexiform layer (OPL)/outer nuclear layer (ONL), and subretinal fluid (SRF) were calculated. The correlations between the baseline fluid volumes and best-corrected visual acuity (BCVA), area of disorganization of the retinal inner layers (DRIL), disrupted external limiting membrane (ELM), and disrupted ellipsoid zone (EZ) at 12 months after treatment were assessed.

Results The baseline volume of the inner IRF correlated with poor BCVA at the final visit ($r = 0.52$, $P < .001$) whereas the baseline volume of the outer IRF and SRF volume did not show a significant correlation with BCVA at the final visit ($P = .07$ and $P = .61$, respectively). The improvement in BCVA correlated with the reduction in the baseline volume of the inner IRF and outer IRF ($r = 0.25$, $P = .04$ and $r = 0.36$, $P = .003$), but not with the SRF volume ($P = .59$). The baseline volume of the inner IRF correlated positively with the area of DRIL and the disrupted ELM at the final visit ($r = 0.56$, $P < .001$ and $r = 0.25$, $P = .04$, respectively). Such relationship remained in each quadrant of the macula ($P < .005$ for all quadrants).

Conclusion The baseline volume of the inner IRF correlated with a poor visual outcome, an increased DRIL area, and a more disrupted ELM area in patients with DME after treatment with bevacizumab.

Keywords Diabetic macular edema · Disorganization of retinal inner layers · Inner nuclear layer · Intraretinal fluid · Retinal fluid volume

Introduction

Diabetic macular edema (DME) is the most common cause of vision loss in diabetic retinopathy [1]. The breakdown of the blood-retinal barrier contributes to fluid collection as intraretinal fluid (IRF) and subretinal fluid (SRF), leading to deterioration in vision [2].

Previous studies have attempted to determine the influence of fluids on clinical outcome after treatment with antivascular endothelial growth factor (VEGF). However, conflicting responses have been reported when DME is categorized by its edema pattern or when fluid diameters were measured [3–7]. These inconsistent results could be due to the different approaches used to acquire 3-dimensional structures with a lower dimensional index. In addition, the presence of multiple fluids of various volumes makes it difficult to choose a representative one to measure. Therefore, we speculated that calculating the summed volume of multiple fluids could be more precise to reflect the pathomorphologic status.

In addition to volumetric analysis, the categorization of the fluid along with the horizontal and depth distributions can provide additional information about DME. Horizontally, the density of photoreceptors decreases with distance

Corresponding Author: Hyung Chan Kim

✉ Hyung Chan Kim
eyekim@kuh.ac.kr

[1] Department of Ophthalmology, Konkuk University School of Medicine, Konkuk University Medical Center, 120-1 Neungdong-ro, Gwangjin-gu, Seoul 05030, Republic of Korea

from the center. Therefore, augmenting the volume of fluids in the central area could provide a better correlation with the clinical outcome [8]. The depth distribution of IRF is composed of IRF in the inner nuclear layer (INL) and of IRF in the outer plexiform layer (OPL)/outer nuclear layer (ONL) [9]. However, little is known about the clinical significance of the IRF in each layer.

Disorganization of the retinal inner layers (DRIL) is a known anatomic marker of the inner retina indicating poor visual outcome in DME [10, 11]. Because multiple IRFs are frequently observed in the INL at baseline, we hypothesize that DRIL at the final visit might correlate with the IRF in INL. A disrupted ellipsoid zone (EZ) and the external limiting membrane (ELM) are 2 recognized morphologic factors associated with visual acuity. They are also worth investigating concerning their correlations with fluid volumes.

In this study, we assessed the correlations of baseline volumes of IRF in INL, IRF in OPL/ONL, and SRF with the visual outcomes of patients with DME after bevacizumab treatment. We also tried to optimize the correlation coefficient by weighting the fluid volumes in the central space with a diameter of 1.5 mm. Finally, we investigated the correlations of the baseline fluid volumes with the anatomically disrupted area at the final visit, including the DRIL, ELM, and EZ.

Patients and methods

Patients' data

We retrospectively reviewed the medical records of patients with DME treated at the Department of Ophthalmology, Konkuk University Medical Center between January 2013 and December 2016. This study followed the tenets of the Declaration of Helsinki. It was approved by the institutional review board of Konkuk University (KUH1100049). The inclusion criteria were as follows: type 2 diabetes mellitus; central macular thickness (CMT) > 300 μm shown on spectral-domain optical coherence tomography (SD-OCT); decimal best-corrected visual acuity (BCVA) between 0.1 and 0.8 (Snellen equivalent 20/200–20/25); DME treated with 1 or more intravitreal injections of bevacizumab; and follow-up of at least 12 months. Eyes were excluded if they had previous vitrectomy; laser photocoagulation within the previous 6 months; ocular diseases other than diabetic retinopathy; high myopia (> 6 spherical D); or poor image quality for segmentation. We screened 169 eyes of DME patients treated with bevacizumab injections and excluded 12 eyes with glaucoma, 44 eyes treated with laser photocoagulation within the previous 6 months or previous vitrectomy, and 2 eyes with high myopia. Forty-six eyes were additionally excluded because of poor image qualities for segmentation. The remaining 65 eyes of 58 patients were included. Each patient underwent a complete ophthalmic examination including medical and ocular histories with ophthalmologic examination including BCVA, fundus photography, and SD-OCT using a Spectralis HRA+OCT (Heidelberg Engineering).

All the patients were treated with intravitreal injections of bevacizumab (1.25 mg/0.05 mL, Avastin). Patients received 3 injections at 4-to 6-week intervals, except 7 eyes whose DME was resolved after 1 or 2 injections. Additional injections were given if needed. The final visit was defined as the visit nearest to 12 months after the initial treatment.

Image analyses

The volume scan covered an area of 9 mm x 6 mm. It contained 25 scans spaced at 250 μm. Scans at baseline and at the final visit were selected for the analyses. Whole scans of each eye were exported in JPG format and uploaded into ImageJ software version 1.50 (https://imagej.nih.gov/ij) [12].

The fluids were defined as follows. Inner IRF was defined as a hyporeflective lesion located in the INL. Outer IRF was defined as a hyporeflective lesion located in the OPL and/or ONL. SRF was defined as a hyporeflective area between the neurosensory retina and retinal pigment epithelium (RPE). DRIL was originally defined as the horizontal extent for which any boundaries between the ganglion cell–inner plexiform layer complex, INL, and OPL could not be identified within a 1-mm diameter area [11]. In this study, we modified the definition as the disorganization within a 3-mm area to match with the volumetric analysis of the fluids. ELM was defined as a hyperreflective band beneath the ONL and above the EZ. The EZ was defined as a second hyperreflective band above the RPE.

The volume of fluid within the 3-mm-diameter cylinder was calculated by multiplying the area of fluid of the B-scans in the cylinder by the thickness of the scan. The inner IRFs, outer IRFs, and SRFs within the 13 B-scans were manually segmented using ImageJ (Fig. 1a). These scans were arrayed and thickened to 250 μm to make rectangular blocks (Fig. 1b). Whole blocks were cropped with their boundaries taking the shape of the of 3-mm- and 1.5-mm-diameter cylinders. The B-scans from the middle of these blocks were then extracted (Fig. 1c). From these scans, the volume of fluid was calculated by multiplying the area by 250 μm (Fig. 1d). Because the boundary of the 1.5- and 3-mm cylinders extended only to the middle of the blocks at both ends, the areas of the fluids at both ends were multiplied by 125 μm. All volumes from the 13 blocks were summed to obtain the total volume (Fig. 1e). To analyze the area of DRIL, disrupted ELM, and disrupted EZ at the final visit, the lesions were manually lined to 1 pixel in thickness. The areas of these lesions within the 1.5-mm- and

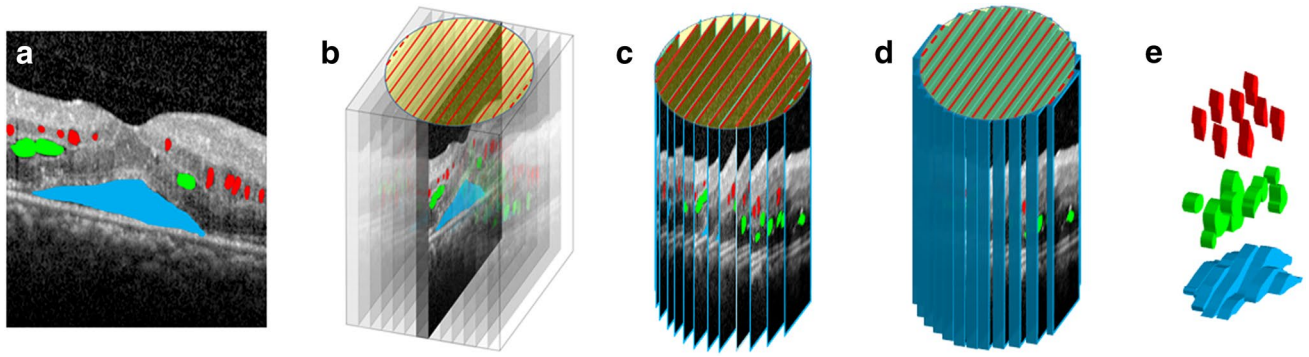

Fig. 1 Construction of 3-dimensional volume of fluid and calculation of the volume from optical coherence tomography B-scans. **a** Intraretinal fluids (IRFs) in the inner nuclear layer (red color), IRFs in the outer plexiform layer/outer nuclear layer (green color), and subretinal fluid (blue color) were manually segmented. **b** The thickness of each scan was lengthened to 250 μm. Blocks were cropped into a cylinder with a diameter of 3 mm (circle on the top). **c** Thirteen B-scans were selected from the cylinder, each of which was spaced 250 μm apart. **d** To obtain the volume of the fluids, their areas were multiplied by their thicknesses: 250 μm for the central blocks and 125 μm for both ends. **e** The volumes of all 13 blocks were summed to obtain the total volume of each fluid

3-mm-diameter cylinders were calculated in a similar way to that for the calculation of the fluid volume.

Two graders (H.L. and K.E.K.) segmented the lesions in the dataset containing the B-scans from 33 eyes and 32 eyes, respectively. Owing to a limitation of time and effort for manual segentation, the intergrader reliability was tested in 520 B-scans of 20 eyes (1 eye had 13 B-scans at baseline and 13 B-scans at the final visit). Ten eyes from each grader's dataset were randomly selected and gathered. Each grader independently segmented the lesions of these 20 eyes, and the intraclass correlation coefficient (ICC) was calculated for the pixel counts of all the segmented lesions. When the consistency of segmentation was confirmed by the ICC, the remaining eyes in each grader's dataset (23 eyes in the datatset of H.L., 22 eyes in the dataset of K.E.K.) were further segmented by each grader. Finally, the supervisor (H.C.K.) reviewed all the individual segmentations and corrected errors if required with open discussion.

To assess the spatial correlation between the baseline volume of the inner IRF and the area of DRIL at the final visit, the macula area was divided into 4 quadrants: superotemporal, superonasal, inferotemporal, and inferonasal. The correlation was then analyzed for each quadrant.

Weighting of the fluid volume within the central 1.5-mm area

Because the cone photoreceptor density was the highest at the center, the impact of the central fluid was assessed by weighting the volumes within the central 1.5-mm area. The weighting was done by multiplying the original fluid volumes within the central 1.5-mm area 2- and 3-fold. The weighted central volume was then added to the outside fluid volume. In addition to the original volume, these weighted volumes of the central area were subjected to correlation analyses to find the one that had the highest correlation with the visual acuity at baseline and at the final visit [8].

Patients groups according to treatment response

A poor responder was defined as eyes with no reduction, a reduction of less than 50 μm, or an increase in central retinal thickness (CMT) at 3 months after the initial anti-VEGF injection as compared with baseline. A good responder was defined as the group of eyes that did not fulfill the criteria for poor responders. Because the enrolled patients were treated on an as-needed basis, the number of injections differed according to each patient's status.

Statistical analyses

Statistical analyses were performed using SPSS version 18.0 (SPSS). Snellen visual acuity was converted to logarithm of the minimal angle of resolution (logMAR) BCVA for the statistical analyses. Probability values less than .05 were considered significant. The ICC was calculated for the volumes and areas of the manually segmented lesions assessed by the 2 graders. The Pearson correlation coefficient was calculated to assess the relationship between the fluid volume and the BCVA. Changes in the values after treatment were evaluated using a paired *t* test. The Mann-Whitney test was performed to compare the parameters between the good responders and the poor responders. To find the visual prognostic factor, baseline factors that showed significant correlation with the final visual acuity on univariable regression analysis were entered into multivariable regression analysis in a stepwise manner.

Results

Patients' characteristics

This study included 65 eyes of 58 patients whose average age was 57.9 ± 11.5 years with a mean follow-up period of 13.9 ± 1.8 months (range, 12–18 months). The mean logMAR BCVA at baseline was 0.34 ± 0.24 and the mean number of bevacizumab injections was 3.8 ± 1.4. The mean durations of DM and hypertension were 14.2 ± 8.6 years and 6.1 ± 8.1 years, respectively. The mean glycated hemoglobin (HbA1C [%]) level at baseline was 8.1 ± 1.8. Regarding the grade of diabetic retinopathy at baseline, 4 patients (6.2%) had mild NPDR; 8 (12.3%), moderate NPDR; 18 (27.7%), severe NPDR; and 35 (53.8%),PDR.

Fluid characteristics and visual acuity at baseline

The ICC for all segmented lesions between the 2 graders was 0.90 ($P = .01$). At baseline, inner IRF, outer IRF, and SRF within a 3-mm area were observed in 57 (87.7%), 63 (96.9%), and 28 (43.1%) eyes, respectively. The mean fluid volumes of inner IRF, outer IRF, total IRF, and SRF within a 3-mm area at baseline were 0.04, 0.21, 0.25, and 0.04 mm^3, respectively (Table 1).

The mean outer IRF volume was significantly higher than the mean inner IRF volume and SRF volume at baseline (both $P < .001$). No significant difference was found between the mean inner IRF volume and the mean SRF volume at baseline ($P = .85$).

The baseline BCVA was poorer than the BCVA at the final visit (Table 1). A positive correlation was found between the baseline BCVA and the final BCVA ($r = 0.58$, $P < .001$). The poorer baseline BCVA correlated with the larger baseline volumes of inner IRF, outer IRF, and total IRF within a 3-mm area ($r = 0.48$, $P < .001$; $r = 0.40$, $P = .001$; $r = 0.47$, $P < .001$, respectively), but not of SRF ($r = -0.01$, $P = .97$).

Correlation of fluid volumes at baseline with visual acuity at the final visit

The baseline volume of inner IRF within a 3-mm area significantly correlated with the BCVA at the final visit ($r = 0.52$, $P < .001$), whereas the baseline volume of outer IRF did not ($r = 0.23$, $P = .07$) (Fig. 2a, 2b). The total IRF volume within a 3-mm area at baseline also correlated with the BCVA at the final visit, while the baseline SRF volume did not ($r = 0.32$, $P = 0.01$ and $r = 0.07$, $P = .61$, respectively) (Fig. 2c, d).

Table 1 Parameters at baseline and at the final visit

Factors	Baseline	Final visit	*P*
BCVA, logMAR	0.34 ± 0.24	0.26 ± 0.23	.002
Volume of fluids, mm^3			
Within 3-mm area			
Inner IRF	0.04 ± 0.05	0.04 ± 0.07	.66
Outer IRF	0.21 ± 0.22	0.07 ± 0.11	.001
Total IRF	0.25 ± 0.24	0.10 ± 0.14	.001
SRF	0.04 ± 0.18	0.002 ± 0.01	.048
Within 1.5-mm area			
Inner IRF	0.02 ± 0.04	0.02 ± 0.05	.81
Outer IRF	0.10 ± 0.12	0.03 ± 0.05	.001
Total IRF	0.13 ± 0.12	0.05 ± 0.08	.001
SRF	0.03 ± 0.08	0.002 ± 0.009	.003
Area, mm^2			
DRIL	-	0.13 ± 0.25	-
Disrupted ELM	-	0.54 ± 0.83	-
Disrupted EZ	-	0.99 ± 1.18	-

BCVA best corrected visual acuity, *logMAR* logarithm of the minimal angle of resolution, *inner IRF* intraretinal fluid volume in the inner nuclear layer at baseline, *outer IRF* intraretinal fluid volume in the outer plexiform layer/outer nuclear layer at baseline, *SRF* subretinal fluid at baseline, *DRIL* disorganization of the retinal inner layers, *ELM* external limiting membrane, *EZ* ellipsoid zone

Means ± standard deviations are depicted

Weighting the volume of the inner IRF at baseline at the central 1.5-mm area as 2-fold or 3-fold did not improve its correlation with the BCVA at the final visit ($r = 0.50$, $P < .001$ and $r = 0.48$, $P < .001$, respectively). Weighting the outer IRF volume at baseline in the central area showed that it was not significantly correlated with the final BCVA ($r = 0.22$, $P = .08$ and $r = 0.12$, $P = .07$). Meanwhile, the baseline BCVA correlated significantly with the BCVA at the final visit ($r = 0.58$, $P < .001$).

We performed a multivariable regression analysis on the BCVA at the final visit using baseline factors including baseline BCVA and volumes of inner IRF, outer IRF, total IRF, and SRF within a 3-mm area. The final BCVA was improved when the baseline BCVA was better and the inner IRF volume at baseline was smaller ($R^2 = 0.42$, $P < .001$; Table 2).

Change in fluid volume and its association with change in visual acuity

The presence of inner IRF, outer IRF, and SRF within the 3-mm area was reduced in 47 (72.3%), 51 (78.5%), and 5 (7.7%) eyes, respectively, at the final visit. The mean volumes of outer IRF and SRF within the 3-mm area were also reduced at the final visit ($P < .001$ and $P = .04$, respectively), whereas the inner IRF volume was not significantly changed ($P = .66$; Table 1).

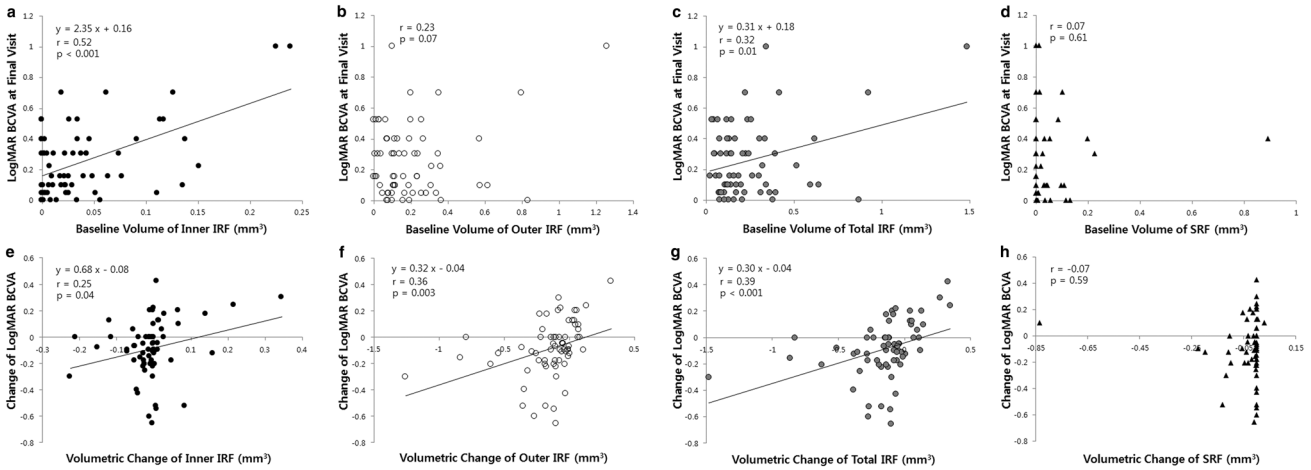

Fig. 2 Scatterplots showing correlations between fluid volumes at baseline and visual acuities at the final visit. The line of best fit is drawn when there is a significant correlation. **a** Volumes of baseline inner intraretinal fluid (IRF) in the inner nuclear layer (INL) within the 3-mm area correlated with the minimal angle of resolution (logMAR) best-corrected visual acuity (BCVA) at the final visit (r = 0.52, P < .001). **b** The baseline volume of the outer IRF in the outer plexiform layer (OPL)/outer nuclear layer (ONL) within the 3-mm area did not correlate with the logMAR BCVA at the final visit (r = 0.23, P = .07). **c** The total baseline IRF volume within the 3-mm area correlated with the logMAR BCVA at the final visit (r = 0.32, P = .01). **d** The subretinal fluid (SRF) volume at baseline did not correlate with the logMAR BCVA at the final visit (r = 0.07, P = .61). **e** Volumetric change in the inner IRF within the 3-mm area correlated with the change in the logMAR BCVA (r = 0.25, P = .04). **f** The volumetric change in the outer IRF within the 3-mm area correlated with the change in the logMAR BCVA (r = 0.36, P = .003). **g** The volumetric change in the total IRF within the 3-mm area correlated with the change in the logMAR BCVA (r = 0.39, P < .001). **h** The volumetric change in the SRF within the 3-mm area did not correlate with the change in the logMAR BCVA (r = -0.07, P = .59)

Table 2 Baseline factors associated with the final BCVA as shown by multivariate regression analysis

Baseline factors	Standardized beta	*P*
BCVA, logMAR	0.41	< .001
Inner IRF	0.33	.004
Outer IRF	N/A	N/A
Total IRF	N/A	N/A
SRF	N/A	N/A
Age	0.19	.05
Sex	-0.08	.39

BCVA best corrected visual acuity, *logMAR* logarithm of the minimal angle of resolution, *inner IRF* intraretinal fluid volume in the inner nuclear layer at baseline, *outer IRF* intraretinal fluid volume in the outer plexiform layer/outer nuclear layer at baseline, *SRF* subretinal fluid volume at baseline, *N/A* not applicable owing to elimination from the stepwise multivariate regression analysis

Adjusted for age and sex

The mean change in the logMAR BCVA after treatment was -0.09 ± 0.22. The improvement in BCVA was associated with reduction in both the inner and the outer IRF volumes within the 3-mm area (r = 0.25, P = .04 and r = 0.36, P = .003, respectively; Fig. 2e, f). The reduction in the total IRF volume within the 3-mm area had the highest correlation with improvement in BCVA (r = 0.39, P < .001; Fig. 2g). The change in the SRF volume within the 3-mm area did not correlate significantly with the change in BCVA (r = -0.07, P = .59; Fig. 2h).

Fluid volumes at baseline according to treatment reponse

The good responder group comprised 38 eyes (58.5%), while the poor responder group comprised 27 eyes (41.5%). When we compared the morphologic parameters at baseline and at the final visit between the good and the poor responder groups, the baseline inner IRF volume within the 3-mm area did not differ significantly between the 2 responder groups (good vs poor: 0.05 mm^3 vs 0.03 mm^3; P = .39). On the other hand, in the good responder group, the baseline volumes of the outer IRF, total IRF, and SRF within the 3-mm area were higher than those of the poor responder group (good vs poor: 0.26 mm^3 vs 0.14 mm^3, P = .048; 0.30 mm^3 vs 0.17 mm^3, P = .04; 0.07 mm^3 vs 0.01 mm^3, P = .02; respectively).

The visual acuity at baseline or at the final visit did not differ significantly between the 2 groups (0.39 vs 0.28, P = .08 and 0.25 vs 0.26, P = .50, respectively).

Anatomic changes at the final visit and their association with fluid volumes at baseline

The DRIL area at the final visit did not correlate significantly with the area of disrupted ELM or EZ at the final

visit ($r = 0.19$, $P = .13$ and $r = 0.20$, $P = .11$, respectively). The BCVA at the final visit correlated significantly with the areas of all 3 lesions (DRIL, disrupted ELM, and disrupted EZ) at the final visit ($r = 0.43$, $P < .001$; $r = 0.39$, $P = .001$; $r = 0.44$, $P < .001$, respectively).

The baseline volume of the inner IRF within the 3-mm area was associated with the area of DRIL at the final visit and with the area of disrupted ELM at the final visit (Table 3). However, its correlation with the area of EZ at the final visit was not significant (Table 3). The volume of outer IRF within the 3-mm area at baseline did not correlate significantly with any anatomic changes, including the DRIL, ELM, and EZ (Table 3). The total IRF volume within the 3-mm area at baseline was associated with the area of DRIL, but not with the area of disrupted ELM or EZ, at the final visit (Table 3). The volume of SRF within the 3-mm area at baseline did not correlate significantly with any anatomic changes in the areas of the DRIL, ELM, or EZ (Table 3). Representative cases are depicted in Figure 3.

When the 3-mm area was divided into quadrants, the baseline inner IRF volume in each quadrant correlated with the DRIL area at the final visit (superotemporal: $r = 0.34$, $P = .004$; superonasal: $r = 0.44$, $P < .001$; inferotemporal: $r = 0.38$, $P = .002$; inferonasal: $r = 0.39$, $P = .002$, respectively).

Discussion

We investigated the effect of 3-dimensionally quantified fluids on visual acuity and anatomic change in DME. To analyze the characteristics of the multiple, 3-dimensionally distributed fluids more precisely, we summed the volumes of the fluids within the macula and assessed their effect on the visual and anatomic outcomes at 1 year after treatment with bevacizumab. In addition, we assessed the effect of IRF volume at baseline on the visual outcome by dividing it into 2 categories according to their location: INL and OPL/ONL. Byeon and colleagues [13] investigated the OCT findings of focal and diffuse DME identified on fluorescein angiography. A diffuse leakage pattern revealed that IRF was located in the INL. The authors postulated that this IRF came from the deep capillary plexus. On the other hand, a focal leakage pattern usually indicated IRF in the OPL/ONL. This fluid was suggested to originate from microaneurysms. It was reported in another study that the height of IRF in ONL is negatively associated with BCVA at the same time point [14]. These characteristics of IRF in the inner and outer layers prompted us to hypothesize that the volumes of inner and outer IRF at baseline could have different clinical impacts.

Our results revealed that the inner IRF volume within the 3-mm area at baseline correlated with the final BCVA, while the outer IRF at baseline did not. The volume of the total IRF at baseline equivalent to conventional IRF significantly correlated with the final BCVA. However, the volume of the total IRF within the 3-mm area at baseline did not remain significant in the multivariable regression model for final visual outcome. Therefore, previous conflicting results about the effect of IRF on visual outcome could be attributed to the varied ratios of inner IRF to outer IRF as well as to the nonvolumetric approach. On the basis of these results, the inner IRF volume at baseline can be used as a new prognostic factor for visual outcome in DME.The negative effect of the inner IRF volume at baseline on visual outcome can be explained by damage to the bipolar cell body: bipolar cells can connect the signal from photoreceptors to ganglion cells and their mechanical stretching by IRF formation could result in dysfunction of the cell body, as suggested in a previous study using microscopic data [15]. Because the cell body of the bipolar cell resides in the INL, increased IRF volume in the INL can damage the cell body. Given the absence of correlation between the baseline outer IRF volume and the final BCVA, damage to the axon is supposed to be more reversible when the cell body is not directly damaged . In addition, the damaging effect by the inner IRF at baseline did not seem to be permanently detrimental to visual function because the BCVA was improved according to the reduction in the inner IRF volume in our correlation analysis with marginal significance ($P = .04$). However, this result was not considered to be clinically significant because

Table 3 Correlation of fluid volumes at baseline with visual acuity-associated parameters at the final visit

Baseline factors	DRIL		Disrupted ELM		Disrupted EZ	
	r	*P*	r	*P*	r	*P*
Inner IRF	0.56	< .001	0.25	.04	0.20	.12
Outer IRF	0.22	.08	-1.16	.22	-0.12	.33
Total IRF	0.32	.01	-0.08	.53	-0.03	.84
SRF	-0.09	.49	0.07	.60	0.10	.42

Inner IRF intraretinal fluid volume in the inner nuclear layer at baseline, *outer IRF* intraretinal fluid volume in the outer plexiform layer/outer nuclear layer at baseline, *SRF* subretinal fluid volume at baseline, *DRIL* area of disorganization of the retinal inner layers *disrupted ELM* area of disrupted external limiting membrane, *disrupted EZ* area of disrupted ellipsoid zone

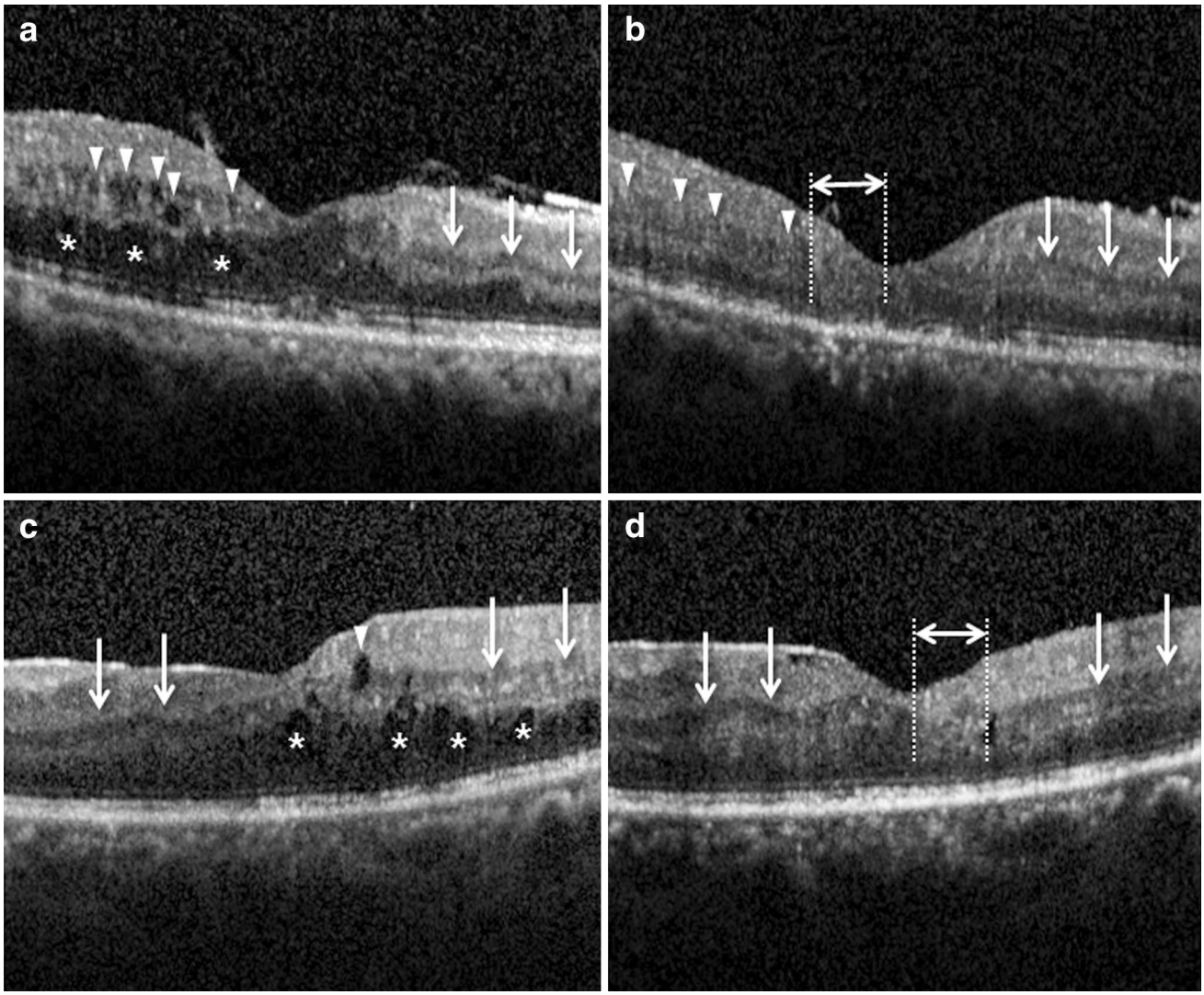

Fig. 3 Two cases showing an association between the baseline inner intraretinal fluid (IRF) in the inner nuclear layer (INL) and disorganization of the retinal inner layers (DRIL) at the final visit on optical coherence tomography. **a** Right eye of a 60-year-old woman whose initial BCVA was 20/80. At baseline, the inner IRF (arrow heads) and outer IRF in the outer nuclear layer (ONL) (asterisks) were prominent on the left side of the fovea in comparison with the right side (arrows). **b** At 12 months after 4 injections of bevacizumab, the upper and lower margins of the INL on the left side of the fovea were vague (arrow heads) and completely disorganized (between dashed lines) when compared with the right side (arrows). The final visual acuity was 20/200. **c** Another case showing the right eye of a 48-year-old man. The initial BCVA was 20/25. Inner IRF (arrow heads) and multiple outer IRFs (asterisks) were present on the right side of the fovea. A relatively intact margin of the ONL was observed (arrows). **d** At 12 months after 5 injections of bevacizumab, the upper and lower margins of the INL were smudged in the location where the inner IRF previously existed (between dashed lines) when compared with the perifoveal area (arrows). The final visual acuity was 20/30

the mean change in the inner IRF volume in all the patients was not significant ($P = .66$).

Next, we tested whether accentuation of the baseline IRF volume in the central 1.5-mm area could enhance the predictive power for the visual prognosis because the density of cone cells is highest at the foveal center. However, weighting of the central volume of the inner IRF did not improve the correlation with BCVA, indicating that the impact of the inner IRF within the 1.5-mm area was not more significant than that within the perifoveal area, which was contrary to what we had expected. This feature seems to be specific to DME because a similar approach on age-related macular degeneration has shown that the predictive power could be increased by augmenting the fluid volume of the central area [8]. Fluid lesions within the 3-mm area in DME might be distributed more evenly than in AMD, in which the pathologic lesions are more focused in the central foveal area. Therefore, weighting the fluid volume within the 1.5-mm area in DME might not play a significant role in augmenting the effect of the total fluid, leading to no significant

difference being found in the results between weighting and not weighting.

The visual acuity at the final visit and the inner IRF volume within the 3-mm area at baseline did not differ significantly between the good and the poor responders. Therefore, the division of patients based on CMT reduction is not thought to reflect the final visual acuity, or its associated baseline factor—inner IRF volume. This discrepancy between change in CMT and final visual outcome has also been found in previous studies [16, 17]. Therefore, we thought that quantitative investigation of the subcomponents of the pathologic changes such as inner IRF, outer IRF, and SRF instead of CMT could provide more information about the association between the structural change in the retina at baseline and the visual outcome after treatment.

The DRIL area at the final visit was associated with the baseline volume of the inner IRF within the 3-mm area. The DRIL was defined as the presence of a region on the B-scan of OCT where the boundaries between the ganglion cell and inner plexiform layer complex, inner nuclear layer, and outer plexiform layer could not be separately identified, and the DRIL was associated with poor visual outcome in DME [11, 18]. The vague retinal layer boundary of the DRIL at the final visit is thought to represent anatomically disrupted cells that participate in the visual transmission pathway [11, 19]. While no histologic evidence exists to support this hypothesis, recent prospective studies have intensified the clinical implication of DRIL as an OCT marker associated with visual outcome [20, 21]. The INL is a common location shared by both the DRIL and the inner IRF. The development of inner IRF in the INL could induce mechanical damage to the adjacent cells and eventually disrupt the boundaries around the INL in OCT, resulting in DRIL at the final visit. Moreover, the correlation between the inner IRF volume at baseline and the DRIL area in each macular quadrant at the final visit showed their spatial association in addition to their quantitative relationship shown above. However, it was hard to conclude that the inner IRF at baseline contributed to poor visual outcome through the formation of DRIL at the final visit because we did not analyze the DRIL at baseline owing to the difficulty in discriminating the DRIL from coarse backgrounds containing hard exudates and inner IRFs at baseline. Nevertheless, the inner IRF volume at baseline still has an advantage in helping to predict visual outcome and the area of DRIL at the final visit because the boundary of the inner IRF is easier to be segmented than that of DRIL in edematous retina. OCT with a higher resolution might enable segmentation of DRIL at baseline with reliability, disclosing the contribution of baseline DRIL and inner IRF to the formation of DRIL more clearly.

In addition, the baseline inner IRF volume within the 3-mm area correlated with the disrupted ELM area, but not with the disrupted EZ area at the final visit. The ELM is the junctional complex between Müller cells and photoreceptors [22, 23]. It maintains the integrity of the photoreceptors' inner segments by forming a diffusion barrier between the subretinal space and the inner retina. Disturbance of the ELM might lead to an imbalance in the oncotic pressure or protein gradient, allowing neurotoxic blood constituents to translocate to the subretinal spaces with concomitant exacerbation of photoreceptor dysfunction. For this reason, we can speculate why the disrupted ELM could be a good predictor of poor visual outcome even though the ELM is not associated with direct damage to the photoreceptors [24]. The EZ is the inner segment ellipsoid zone containing densely packed mitochondria that support energy consumption of photoreceptors [25]. For this reason, a disrupted EZ is thought to be directly associated with poor visual outcome [26, 27]. The insignificant correlation between the inner IRF and EZ can be interpreted as a weakened negative influence on the EZ because the EZ is farther than the ELM from the pathologic environment associated with the inner IRF.

This study has several limitations. First, the region of interest was confined to a 3-mm area only. The volume of fluids outside the 3-mm ring could have also affected the visual and anatomic outcomes. Second, the wide spacing of the B-scans (250 μm) could not fully reflect the real morphology of the lesion. Denser B-scans are needed to better describe these lesions. Third, manual delineation is a time-consuming process. An artificial intelligence algorithm that can segment these lesions automatically will reduce the time needed for volume calculation. Finally, the retrospective nature of this study and the small number of patients are limitations. For a better result, a prospective study with larger data will be required.

In conclusion, an increased volume of IRF in the INL at baseline is negatively associated with visual acuity after anti-VEGF treatment in DME. Also, we can anticipate an increased DRIL area after treatment from the volume of IRF in the INL at baseline.

Acknowledgments Professional medical English editing was done by Harrisco English Editing Service.

Conflicts of interest H. Lee, None; K. E. Kang, None; H. Chung, None; H. C. Kim, None.

References

1. Varma R, Bressler NM, Doan QV, Gleeson M, Danese M, Bower JK, et al. Prevalence of and risk factors for diabetic macular edema in the United States. JAMA Ophthalmol. 2014;132:1334–40.
2. Bhagat N, Grigorian RA, Tutela A, Zarbin MA. Diabetic macular edema: pathogenesis and treatment. Surv Ophthalmol. 2009;54:1–32.

3. Kim M, Lee P, Kim Y, Yu SY, Kwak HW. Effect of intravitreal bevacizumab based on optical coherence tomography patterns of diabetic macular edema. Ophthalmologica. 2011;226:138–44.
4. Koytak A, Altinisik M, Sogutlu Sari E, Artunay O, Umurhan Akkan JC, Tuncer K. Effect of a single intravitreal bevacizumab injection on different optical coherence tomographic patterns of diabetic macular oedema. Eye (Lond). 2013;27:716–21.
5. Roh MI, Kim JH, Kwon OW. Features of optical coherence tomography are predictive of visual outcomes after intravitreal bevacizumab injection for diabetic macular edema. Ophthalmologica. 2010;224:374–80.
6. Sophie R, Lu N, Campochiaro PA. Predictors of functional and anatomic outcomes in patients with diabetic macular edema treated with ranibizumab. Ophthalmology. 2015;122:1395–401.
7. Itoh Y, Petkovsek D, Kaiser PK, Singh RP, Ehlers JP. Optical coherence tomography features in diabetic macular edema and the impact on anti-vegf response. Ophthalmic Surg Lasers Imaging Retina. 2016;47:908–13.
8. Waldstein SM, Philip AM, Leitner R, Simader C, Langs G, Gerendas BS, et al. Correlation of 3-dimensionally quantified intraretinal and subretinal fluid with visual acuity in neovascular age-related macular degeneration. JAMA Ophthalmol. 2016;134:182–90.
9. Otani T, Kishi S. Correlation between optical coherence tomography and fluorescein angiography findings in diabetic macular edema. Ophthalmology. 2007;114:104–7.
10. Radwan SH, Soliman AZ, Tokarev J, Zhang L, van Kuijk FJ, Koozekanani DD. Association of disorganization of retinal inner layers with vision after resolution of center-involved diabetic macular edema. JAMA Ophthalmol. 2015;133:820–5.
11. Sun JK, Lin MM, Lammer J, Prager S, Sarangi R, Silva PS, et al. Disorganization of the retinal inner layers as a predictor of visual acuity in eyes with center-involved diabetic macular edema. JAMA Ophthalmol. 2014;132:1309–16.
12. Schneider CA, Rasband WS, Eliceiri KW. NIH Image to ImageJ: 25 years of image analysis. Nat Methods. 2012;9:671–5.
13. Byeon SH, Chu YK, Hong YT, Kim M, Kang HM, Kwon OW. New insights into the pathoanatomy of diabetic macular edema: angiographic patterns and optical coherence tomography. Retina. 2012;32:1087–99.
14. Reznicek L, Cserhati S, Seidensticker F, Liegl R, Kampik A, Ulbig M, et al. Functional and morphological changes in diabetic macular edema over the course of anti-vascular endothelial growth factor treatment. Acta Ophthalmol. 2013;91:e529–36.
15. Pelosini L, Hull CC, Boyce JF, McHugh D, Stanford MR, Marshall J. Optical coherence tomography may be used to predict visual acuity in patients with macular edema. Investig Ophthalmol Vis Sci. 2011;52:2741–8.
16. Wells JA, Glassman AR, Ayala AR, Jampol LM, Bressler NM, Bressler SB, et al. Aflibercept, bevacizumab, or ranibizumab for diabetic macular edema: two-year results from a comparative effectiveness randomized clinical trial. Ophthalmology. 2016;123:1351–9.
17. Maturi RK, Glassman AR, Liu D, Beck RW, Bhavsar AR, Bressler NM, et al. Effect of adding dexamethasone to continued ranibizumab treatment in patients with persistent diabetic macular edema: a DRCR network phase 2 randomized clinical trial. JAMA Ophthalmol. 2018;136:29–38.
18. Das R, Spence G, Hogg RE, Stevenson M, Chakravarthy U. Disorganization of inner retina and outer retinal morphology in diabetic macular edema. JAMA Ophthalmol. 2018;136:202–8.
19. Murakami T, Yoshimura N. Structural changes in individual retinal layers in diabetic macular edema. J Diabetes Res. 2013;2013:920713.
20. Fickweiler W, Schauwvlieghe AME, Schlingemann RO, Maria Hooymans JM, Los LI, Verbraak FD. Predictive value of optical coherence tomographic features in the Bevacizumab and Ranibizumab in Patients with Diabetic Macular Edema (BRDME) Study. Retina. 2018;38:812–9.
21. Santos AR, Costa MÂ, Schwartz C, Alves D, Figueira J, Silva R, et al. Optical coherence tomography baseline predictors for initial best-corrected visual acuity response to intravitreal anti-vascular endothelial growth factor treatment in eyes with diabetic macular edema: the CHARTRES Study. Retina. 2018;38:1110–9.
22. Uga S, Smelser GK. Electron microscopic study of the development of retinal Mullerian cells. Investig Ophthalmol. 1973;12:295–307.
23. Bunt-Milam AH, Saari JC, Klock IB, Garwin GG. Zonulae adherentes pore size in the external limiting membrane of the rabbit retina. Investig Ophthalmol Vis Sci. 1985;26:1377–80.
24. Muftuoglu IK, Mendoza N, Gaber R, Alam M, You Q, Freeman WR. Integrity of outer retinal layers after resolution of central involved diabetic macular edema. Retina. 2017;37:2015–24.
25. Spaide RF, Curcio CA. Anatomical correlates to the bands seen in the outer retina by optical coherence tomography: literature review and model. Retina. 2011;31:1609–19.
26. Maheshwary AS, Oster SF, Yuson RM, Cheng L, Mojana F, Freeman WR. The association between percent disruption of the photoreceptor inner segment-outer segment junction and visual acuity in diabetic macular edema. Am J Ophthalmol. 2010;150:63–7.
27. Shin HJ, Lee SH, Chung H, Kim HC. Association between photoreceptor integrity and visual outcome in diabetic macular edema. Graefes Arch Clin Exp Ophthalmol. 2012;250:61–70.